

Electronic Supplementary Information

Formation and reactivity of an (alkene)peroxoiridium(III) intermediate supported by an amidinato ligand

Matthew R. Kelley and Jan-Uwe Rohde*

Department of Chemistry, The University of Iowa, Iowa City, IA 52242

Contents	Page
Table S1. Additional crystal and data collection parameters for 1	S2
Table S2. Selected interatomic distances for 1	S2
Table S3. Selected angles for 1	S3
Table S4. Selected dihedral angles for 1	S3
Figure S1. High-resolution electron impact ionization mass spectrum of 2	S4
Figure S2. Solid-state IR spectrum 2	S4
Figure S3. ^1H , ^1H COSY spectrum of 3	S5
Figure S4. ^1H , ^{13}C HSQC spectrum of 3	S6
Table S5. ^1H and ^{13}C chemical shifts from the ^1H , ^{13}C HSQC spectrum of 3	S6
Determination of the Self-Diffusion Coefficients of 1 and 3	S7
Figure S5. Plots of $\ln(I/I_0)$ as a function of G^2 for 1 and 3	S8
Figure S6. Solid-state IR spectra of 1 , 3 , 3 - $^{18}\text{O}_2$, and the decay products of 3 and 3 - $^{18}\text{O}_2$	S9
Table S6. IR absorption bands of 2 and 3 (2200–1200 cm^{-1})	S10
Figure S7. Electronic absorption spectra of 1 and 3 in toluene and the solution during decay of 3	S10
Table S7. Mass spectrometric data of the decay products of 3 and 3 - $^{18}\text{O}_2$	S10

Table S1. Additional crystal and data collection parameters for $[\text{Ir}\{\text{PhNC}(\text{Me})\text{NPh}\}(\text{cod})]$, **1**.

1	
Crystal habit, color	blade, orange
Crystal size	0.27 x 0.07 x 0.01 mm ³
$F(000)$	992
θ range for data collection	2.50 to 25.37°
Limiting indices	$-13 \leq h \leq 13, -13 \leq k \leq 12, -16 \leq l \leq 16$
Completeness to θ	99.3 % ($\theta = 25.37^\circ$)
Max. and min. transmission	0.9473 and 0.2435
Refinement method	Full-matrix least-squares on F^2

Table S2. Selected interatomic distances (Å) for $[\text{Ir}\{\text{PhNC}(\text{Me})\text{NPh}\}(\text{cod})]$, **1**.^a

Molecule A		Molecule B	
Ir1–N1	2.094(6)	Ir2–N3	2.100(6)
Ir1–N2	2.077(7)	Ir2–N4	2.076(7)
Ir1–C15	2.102(8)	Ir2–C37	2.099(8)
Ir1–C16	2.129(9)	Ir2–C38	2.132(9)
Ir1–C19	2.102(8)	Ir2–C41	2.099(8)
Ir1–C20	2.105(8)	Ir2–C42	2.127(8)
N1–C1	1.323(10)	N3–C23	1.336(10)
N1–C2	1.394(10)	N3–C24	1.390(9)
N2–C1	1.339(10)	N4–C23	1.334(10)
N2–C8	1.416(10)	N4–C30	1.426(10)
C1–C14	1.506(10)	C23–C36	1.510(11)
C15–C16	1.429(12)	C37–C38	1.421(12)
C19–C20	1.398(12)	C41–C42	1.418(12)

^a Numbers in parentheses are standard uncertainties in the last significant figures. Atoms are labeled as indicated in Figure 1.

Table S3. Selected angles (°) for [Ir{PhNC(Me)NPh}(cod)], **1**.^a

Molecule A		Molecule B	
N2–Ir1–N1	62.7(3)	N4–Ir2–N3	62.8(2)
N1–Ir1–C15	102.0(3)	C37–Ir2–N3	102.7(3)
N1–Ir1–C16	107.2(3)	N3–Ir2–C38	107.6(3)
N1–Ir1–C19	156.1(3)	C41–Ir2–N3	155.0(3)
N1–Ir1–C20	157.1(3)	N3–Ir2–C42	158.1(3)
N2–Ir1–C19	101.3(3)	N4–Ir2–C41	100.8(3)
N2–Ir1–C20	105.2(3)	N4–Ir2–C42	105.6(3)
N2–Ir1–C15	156.0(3)	N4–Ir2–C37	156.0(3)
N2–Ir1–C16	158.3(3)	N4–Ir2–C38	159.1(3)
C15–Ir1–C16	39.5(3)	C37–Ir2–C38	39.2(3)
C19–Ir1–C20	38.8(3)	C41–Ir2–C42	39.2(3)
C15–Ir1–C19	98.4(3)	C37–Ir2–C41	98.5(3)
C15–Ir1–C20	82.1(3)	C37–Ir2–C42	81.0(3)
C19–Ir1–C16	81.2(3)	C41–Ir2–C38	81.1(3)
C20–Ir1–C16	90.3(3)	C42–Ir2–C38	89.1(3)
C1–N1–C2	127.0(7)	C23–N3–C24	127.8(7)
C1–N1–Ir1	93.9(5)	C23–N3–Ir2	93.4(5)
C2–N1–Ir1	138.4(5)	C24–N3–Ir2	138.3(6)
C1–N2–C8	129.4(7)	C23–N4–C30	128.1(7)
C1–N2–Ir1	94.1(5)	C23–N4–Ir2	94.5(5)
C8–N2–Ir1	136.1(5)	C30–N4–Ir2	137.0(5)
N1–C1–N2	109.2(7)	N4–C23–N3	109.1(7)
N1–C1–C14	126.8(7)	N3–C23–C36	126.0(7)
N2–C1–C14	123.9(8)	N4–C23–C36	124.9(8)

^a Numbers in parentheses are standard uncertainties in the last significant figures. Atoms are labeled as indicated in Figure 1.

Table S4. Selected dihedral angles (°) for [Ir{PhNC(Me)NPh}(cod)], **1**.^a

Molecule A		Molecule B	
N1–C1–N2 / N1–Ir1–N2	3.6(8)	N3–C23–N4 / N3–Ir2–N4	4.6(8)
N1–Ir1–N2 / C15–Ir1–C16	82.1(4)	N3–Ir2–N4 / C37–Ir2–C38	82.9(5)
N1–Ir1–N2 / C19–Ir1–C20	83.9(5)	N3–Ir2–N4 / C41–Ir2–C42	82.8(5)
C15–Ir1–C16 / C19–Ir1–C20	87.1(4)	C37–Ir2–C38 / C41–Ir2–C42	86.2(4)
(N1,C1,N2,C14) / (C2→C7) ^b	41.8(4)	(N3,C23,N4,C36) / (C24→C29) ^b	37.6(4)
(N1,C1,N2,C14) / (C8→C13) ^b	54.3(3)	(N3,C23,N4,C36) / (C30→C35) ^b	56.1(3)

^a Numbers in parentheses are standard uncertainties in the last significant figures. Atoms are labeled as indicated in Figure 1. ^b Angle between the least-squares planes of the amidinate atoms (*e.g.*, N1, C1, N2, and C14) and the aryl ring atoms (*e.g.*, C2, C3, C4, C5, C6, and C7).

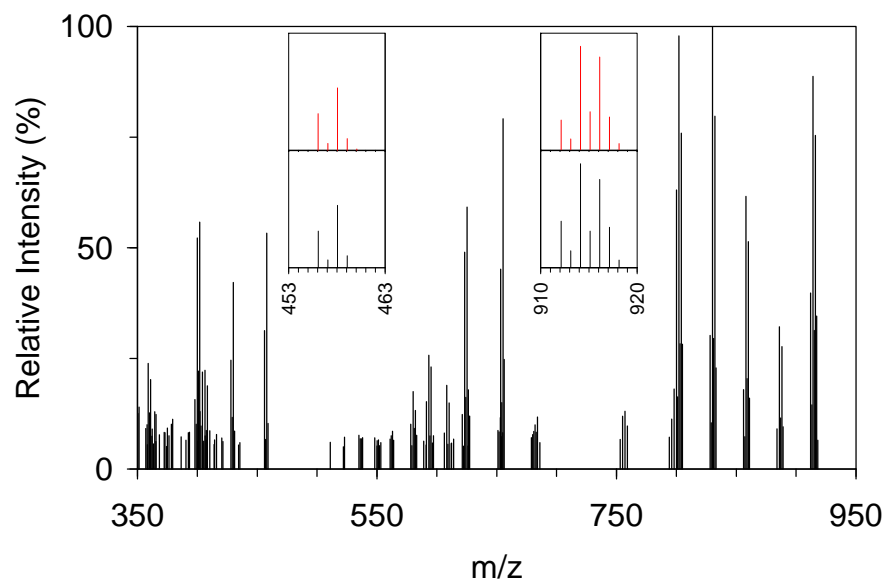


Figure S1. High-resolution electron impact ionization mass spectrum of **2**. Insets: Expanded views of the features attributed to 2^{+} and $\{2/2\}^{++}$ (bottom, —, black) and their calculated isotope distribution patterns (top, —, red).

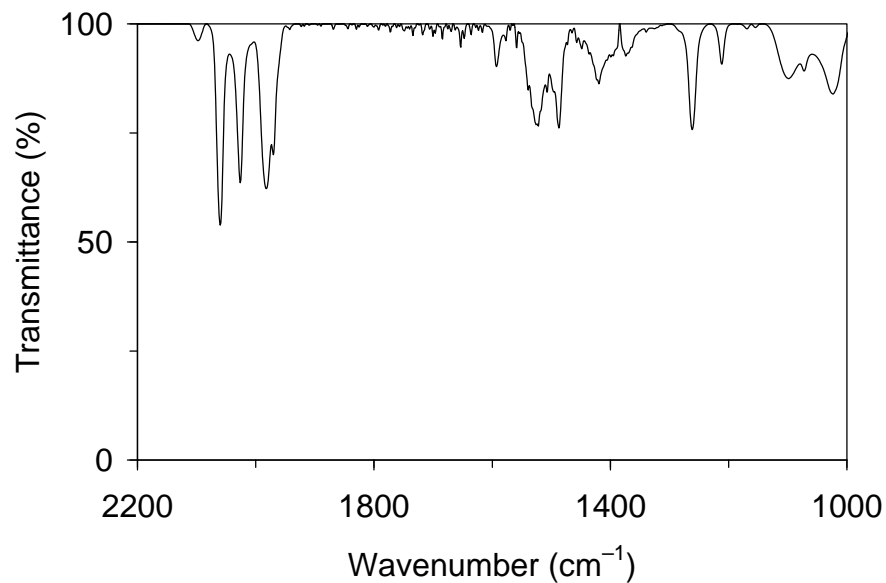


Figure S2. Solid-state IR spectrum (KBr) of **2**.

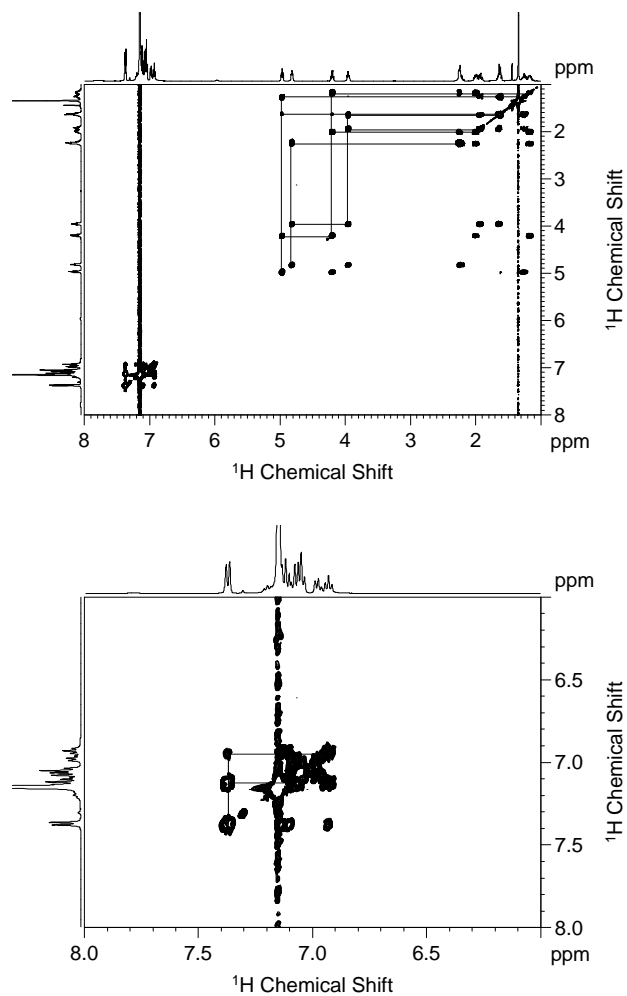


Figure S3. Top: ^1H , ^1H COSY spectrum of **3** in benzene- d_6 (ca. 15 mM, 500 MHz, 25 °C). The solid lines indicate correlations among alkene proton resonances and between alkene and methylene proton resonances. Bottom: Expanded view of the aromatic region of the ^1H , ^1H COSY spectrum of **3**. The solid lines indicate correlations among aromatic proton resonances.

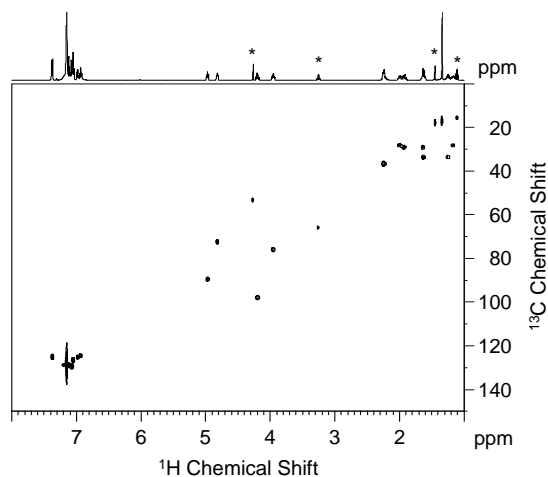


Figure S4. ^1H , ^{13}C HSQC spectrum of **3** in benzene- d_6 (ca. 15 mM, 500 MHz, 25 °C). The asterisks denote solvent peaks (CH_2Cl_2 , Et_2O , and an unknown contaminant).

Table S5. ^1H and ^{13}C chemical shifts, δ (ppm), from the ^1H , ^{13}C heteronuclear single-quantum coherence (HSQC) spectrum of $[\text{Ir}\{\text{PhNC}(\text{Me})\text{NPh}\}\{\text{cod}\}(\text{O}_2)]$ (**3**) in benzene- d_6 .

Assignment		$\delta(^1\text{H})$	$\delta(^{13}\text{C})$
Ar	Group A	7.37	125.1
		7.12 ^a	128.8 ^a
		6.93	124.4
	Group B	7.07	129.4
		7.05	126.5
		6.97	125.2
=CHCH ₂ -	1-H, C-1	4.82	72.4
	2-H, C-2	3.95	75.8
	5-H, C-5	4.97	89.5
	6-H, C-6	4.20	97.8
=CHCH ₂ -	3-H _{ab} , C-3	1.92, 1.64	29.0
	4-H _{ab} , C-4	1.64, 1.26	33.6
	7-H _{ab} , C-7	1.99, 1.17	28.1
	8-H _{ab} , C-8	2.23	36.6
CCH ₃		1.34	17.1

^a The resonance signals centered at $\delta(^1\text{H}) = 7.12$ ppm and $\delta(^{13}\text{C}) = 128.8$ ppm partially overlap with the residual solvent peaks.

Determination of the Self-Diffusion Coefficients of **1** and **3**

Diffusion ^1H NMR experiments to determine D values were conducted in triplicate, and, for each experiment, data of seven (**1**) or ten (**3**) suitable peaks were averaged. The average D values from three measurements were $(8.8 \pm 0.2) \cdot 10^{-10}$ and $(8.3 \pm 0.1) \cdot 10^{-10} \text{ m}^2 \cdot \text{s}^{-1}$ for **1** and **3**, respectively (ca. 17 mM **1** and ca. 15 mM **3** in benzene- d_6 , 400 MHz, 25 °C). Intermediate **3** was found to decay by $\leq 10\%$ over the course of each measurement, introducing a minor error into D . Shown below are representative results for the CCH₃ resonance signals of **1** and **3**. The plots in Figure S5 confirm the expected linear relationship between $\ln(I/I_0)$ and G^2 .

SIMFIT RESULTS for **1**

=====

INTENSITY fit : Diffusion : Variable Gradient :
 $I = I[0] \cdot \exp(-D \cdot \text{SQR}(2 \cdot \text{PI} \cdot \text{gamma} \cdot \text{Gi} \cdot \text{LD}) \cdot (\text{BD} - \text{LD}/3) \cdot 1e4)$
16 points for Peak 6, CCH3 resonance signal
Converged after 32 iterations!

Results Comp. 1
I[0] = 9.998e-001
Diff Con. = 8.704e-010 m2/s
Gamma = 4.258e+003 Hz/G
Little Delta = 5.000m
Big Delta = 26.950m

RSS = 7.767e-006
SD = 6.967e-004

Point	Gradient	Expt	Calc	Difference
1	6.740e-001	1.000e+000	9.980e-001	-1.962e-003
2	2.765e+000	9.696e-001	9.702e-001	5.493e-004
3	4.855e+000	9.101e-001	9.112e-001	1.125e-003
4	6.945e+000	8.262e-001	8.269e-001	6.820e-004
5	9.036e+000	7.254e-001	7.250e-001	-4.898e-004
6	1.113e+001	6.139e-001	6.141e-001	2.269e-004
7	1.322e+001	5.027e-001	5.026e-001	-7.296e-005
8	1.531e+001	3.970e-001	3.975e-001	4.937e-004
9	1.740e+001	3.036e-001	3.037e-001	1.016e-004
10	1.949e+001	2.239e-001	2.241e-001	2.867e-004
11	2.158e+001	1.601e-001	1.599e-001	-2.598e-004
12	2.367e+001	1.111e-001	1.102e-001	-9.175e-004
13	2.576e+001	7.375e-002	7.334e-002	-4.055e-004
14	2.785e+001	4.754e-002	4.718e-002	-3.589e-004
15	2.994e+001	2.946e-002	2.932e-002	-1.381e-004
16	3.203e+001	1.778e-002	1.761e-002	-1.705e-004

=====

SIMFIT RESULTS for **3**

=====

INTENSITY fit : Diffusion : Variable Gradient :
 $I = I[0] \cdot \exp(-D \cdot \text{SQR}(2 \cdot \text{PI} \cdot \text{gamma} \cdot \text{Gi} \cdot \text{LD}) \cdot (\text{BD} - \text{LD}/3) \cdot 1e4)$
16 points for Peak 11, CCH3 resonance signal
Converged after 35 iterations!

Results Comp. 1
I[0] = 1.020e+000
Diff Con. = 8.276e-010 m2/s
Gamma = 4.258e+003 Hz/G
Little Delta = 5.000m
Big Delta = 26.950m

RSS = 6.609e-004
SD = 6.427e-003

Point	Gradient	Expt	Calc	Difference
1	6.740e-001	1.000e+000	1.018e+000	1.838e-002
2	2.765e+000	9.892e-001	9.913e-001	2.142e-003
3	4.855e+000	9.435e-001	9.340e-001	-9.517e-003
4	6.945e+000	8.625e-001	8.516e-001	-1.095e-002
5	9.036e+000	7.600e-001	7.514e-001	-8.534e-003
6	1.113e+001	6.420e-001	6.418e-001	-1.807e-004
7	1.322e+001	5.283e-001	5.304e-001	2.104e-003
8	1.531e+001	4.210e-001	4.243e-001	3.326e-003
9	1.740e+001	3.275e-001	3.285e-001	1.053e-003
10	1.949e+001	2.454e-001	2.461e-001	6.947e-004
11	2.158e+001	1.769e-001	1.785e-001	1.571e-003
12	2.367e+001	1.217e-001	1.253e-001	3.599e-003
13	2.576e+001	8.360e-002	8.508e-002	1.482e-003
14	2.785e+001	5.539e-002	5.593e-002	5.395e-004
15	2.994e+001	3.593e-002	3.558e-002	-3.495e-004
16	3.203e+001	2.194e-002	2.191e-002	-3.130e-005

=====

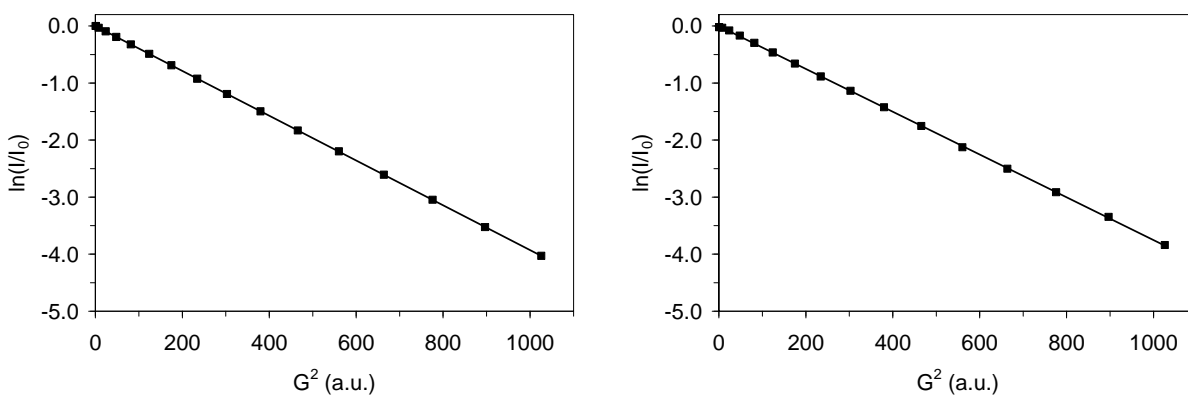


Figure S5. Plots of the natural logarithm of the intensity quotient, $\ln(I/I_0)$, as a function of the square of the gradient strength, G^2 , for the CCH₃ resonance signals of **1** (left; $R^2 = 0.999998$) and **3** (right; $R^2 = 0.999919$) in benzene-*d*₆ (ca. 17 mM **1** and ca. 15 mM **3**, 400 MHz, 25 °C).

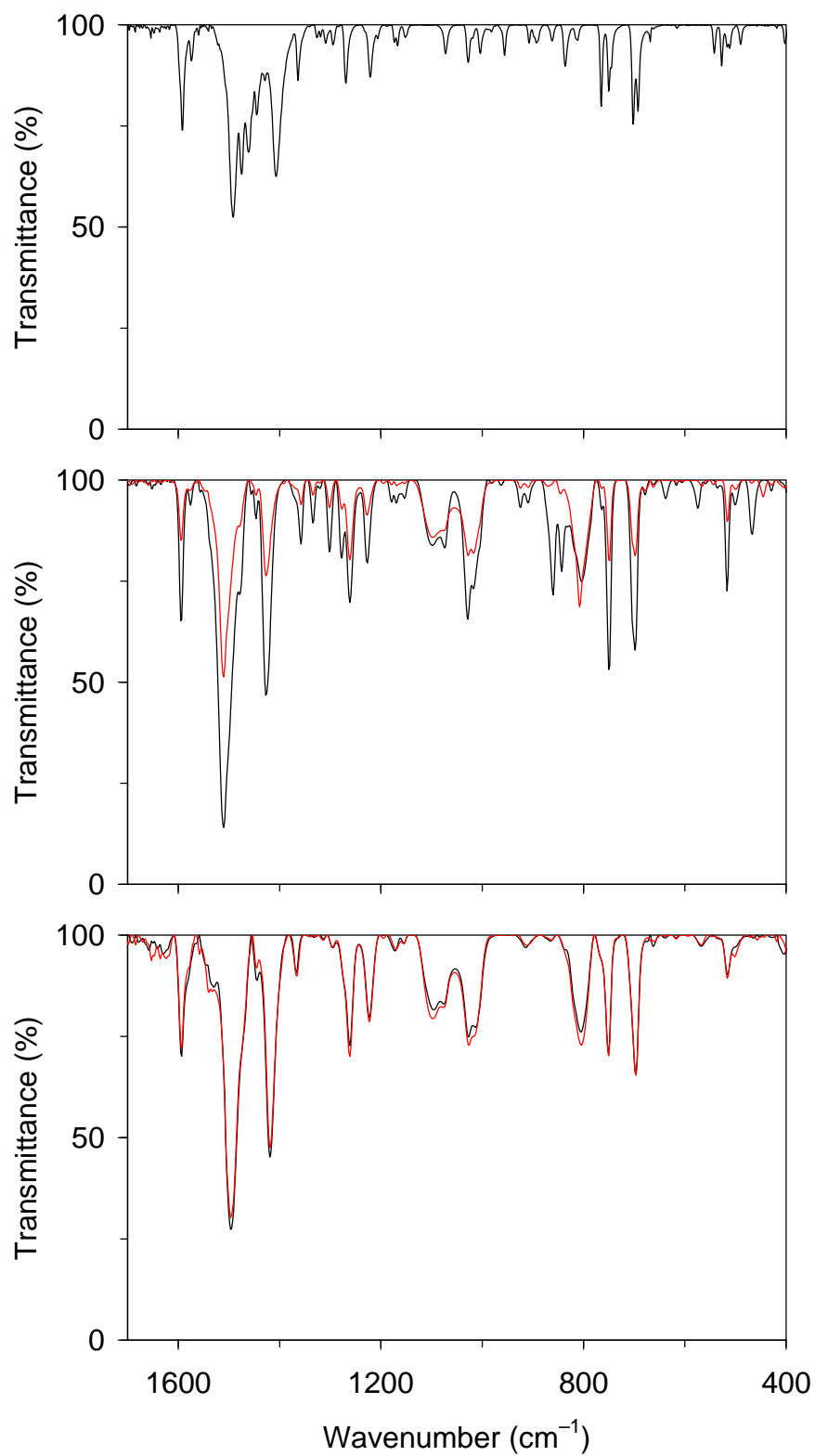


Figure S6. Solid-state IR spectra (KBr) of **1** (top), **3** (middle) and the decay products of **3** (bottom). Spectra of **3**-¹⁸O₂ and its decay products are shown in red (—).

Table S6. IR absorption bands of [$\{\text{Ir}(\text{CO})_2\}_2\{\mu\text{-PhNC}(\text{Me})\text{NPh-}\kappa\text{N}:\kappa\text{N}'\}_2$] (**2**) and [$\text{Ir}\{\text{PhNC}(\text{Me})\text{NPh}\}(\text{cod})(\text{O}_2)$] (**3**) (2200–1200 cm^{-1}).^a

Complex	ν_{CO} (cm^{-1})	ν (cm^{-1})
2	2060 (s), 2026 (s), 1985 (s), 1970 (m)	1593, 1524, 1487, 1419, 1262, 1212
3		1594, 1510, 1479 (sh), 1427, 1358, 1334, 1301, 1277, 1261, 1227

^a Solid state (KBr disk).

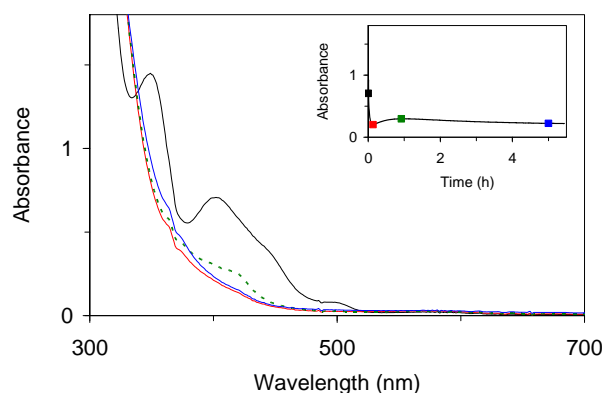


Figure S7. Electronic absorption spectra of 1 mM **1** in toluene at 0 °C (—, black), **3** generated from the reaction of **1** with O_2 (—, red), and the solution during decay of **3** (---, green; and —, blue; path length, 0.5 cm). Inset: Time course of the reaction of **1** in toluene with O_2 at 0 °C and subsequent decay of **3** ($\lambda = 402$ nm). The squares indicate the reaction times associated with the spectra shown (black, **1**; red, **3**; green and blue, solution during decay of **3**).

Table S7. Mass-to-charge ratios (m/z) from the electrospray ionization (ESI) and electron impact (EI) mass spectra of the decay products of [$\text{Ir}\{\text{PhNC}(\text{Me})\text{NPh}\}(\text{cod})(\text{O}_2)$] (**3**).^{a-c}

	ESI(+) MS				EIMS	
	$\{\text{LH} + \text{H}\}^+$	$\{\mathbf{3} - \text{O}_2\text{H}\}^+$	$\{\mathbf{3} - \text{OH}\}^+$	$\{\mathbf{3} - \text{H}\}^+$	$\{\mathbf{3} - \text{H}_2\text{O}\}^{++}$	$\{\text{IrL}_3\}^{++}$
Found	211.2	509.4	525.2	541.2	524.1397	820.2827
Calcd	211.1	509.2	525.2	541.2	524.1440	820.2866
Found ($^{18}\text{O}_2$)	211.3	509.5	527.4	545.4	526.3	820.4

^a The reaction of [$\text{Ir}\{\text{PhNC}(\text{Me})\text{NPh}\}(\text{cod})$] (**1**) with O_2 (or $^{18}\text{O}_2$) was carried out as described in the Experimental Section, and the resulting solution was allowed to stand for at least 16 h. ^b LH = $\text{PhN}=\text{C}(\text{Me})\text{NPh}$.

^c High-resolution mass spectral data are reported with four decimal places.